Matrix Biology 29 (2010) 228–236

Contents lists available at ScienceDirect

Matrix Biology

journal homepage: www.elsevier.com/locate/matbio

Characterizing molecular diffusion in the lens capsule

Brian P. Danysh [a], Tapan P. Patel [a], Kirk J. Czymmek [a,b], David A. Edwards [c], Liyun Wang [d], Jayanti Pande [e], Melinda K. Duncan [a,*]

[a] Department of Biological Sciences, University of Delaware, Newark, DE 19716, USA
[b] Delaware Biotechnology Institute, University of Delaware, Newark, DE 19711, USA
[c] Department of Mathematical Sciences, University of Delaware, Newark, DE 19716, USA
[d] Department of Mechanical Engineering, University of Delaware, Newark, DE 19716, USA
[e] Department of Chemistry, University at Albany, State University of New York, Albany, NY 12222, USA

ARTICLE INFO

Article history:
Received 19 October 2009
Received in revised form 14 December 2009
Accepted 14 December 2009

Keywords:
Lens capsule
Basement membrane
Diffusion coefficient
Permeabilitiy
Binding affinity
Partition coefficient
FRAP

ABSTRACT

The lens capsule compartmentalizes the cells of the avascular lens from other ocular tissues. Small molecules required for lens cell metabolism, such as glucose, salts, and waste products, freely pass through the capsule. However, the lens capsule is selectively permeable to proteins such as growth hormones and substrate carriers which are required for proper lens growth and development. We used fluorescence recovery after photobleaching (FRAP) to characterize the diffusional behavior of various sized dextrans (3, 10, 40, 150, and 250 kDa) and proteins endogenous to the lens environment (EGF, γD-crystallin, BSA, transferrin, ceruloplasmin, and IgG) within the capsules of whole living lenses. We found that proteins had dramatically different diffusion and partition coefficients as well as capsule matrix binding affinities than similar sized dextrans, but they had comparable permeabilities. We also found ionic interactions between proteins and the capsule matrix significantly influence permeability and binding affinity, while hydrophobic interactions had less of an effect. The removal of a single anionic residue from the surface of a protein, γD-crystallin [E107A], significantly altered its permeability and matrix binding affinity in the capsule. Our data indicated that permeabilities and binding affinities in the lens capsule varied between individual proteins and cannot be predicted by isoelectric points or molecular size alone.

1. Introduction

The lens capsule is a relatively thick basement membrane completely encasing the cells of the lens, thus sequestering them from the surrounding aqueous and vitreous humors (Beyer et al., 1984; Cotlier et al., 1968; Karkinen-Jaaskelainen et al., 1975; Danysh et al., 2008). It is multifunctional, protecting the lens epithelial and cortical fiber cells from infectious agents, providing mechanical and structural integrity during lens accommodation, as well as cell signaling during the development and growth of the lens (Danysh and Duncan, 2009; Walker and Menko, 2009). The main structural components of the lens capsule, collagen IV, laminin, nidogen/entactin, and heparan sulfate proteoglycans (HSPGs) (Cammarata et al., 1986; Rossi et al., 2003; Yurchenco et al., 2004), self-assemble into a complex three-dimensional viscoelastic meshwork (Chen and Hansma, 2000; Laurie et al., 1986; Krag and Andreassen, 2003; Yurchenco and Schittny, 1990). While the composition and assembly of the capsule is similar to other basement membranes, including the glomerular basement membrane (GBM), it does differ in the identity and ratio of the isoforms present (Groffen et al., 1998; Mohan and Spiro, 1986).

The basement membrane functions as a molecular sieve modulating the transport of solutes including nutrients, metabolites, and signaling molecules such as cytokines and growth factors. In the kidney, the GBM works together with slit diaphragms and capillary endothelial cells forming the glomerular barrier, restricting the passage of large proteins but allowing water and smaller proteins to pass into the urine (Haraldsson et al., 2008; Smithies, 2003). For the avascular lens, the lens capsule serves as the sole filter for the transit of water, nutrients, waste products, substrate carriers, and cell signaling molecules between the ocular environment and the lens cells (Fels, 1970; Fisher, 1977; Friedenwald, 1930a; Robinson, 2006; Tholozan et al., 2007). Both the GBM and lens capsule have a net negative charge primarily due to an abundance of heparan sulfate glycosaminoglycan (GAG) side chains (Kanwar and Farquhar, 1979a, b; Landemore et al., 1999; Webster et al., 1987; Winkler et al., 2001; Kanwar et al., 1980); but the lens capsule contains several times more GAG side chains (per unit dry tissue weight) than the GBM (Mohan and Spiro, 1986; Parthasarathy and Spiro, 1982). In addition to steric exclusion factors, these negatively charged side chains have been proposed to be responsible for the reduced permeability of proteins through the lens capsule (Friedenwald, 1930b). However, the effect of charge on selective permeability is still controversial in the GBM (Haraldsson et al., 2008; Friedenwald, 1930b; Bray and Robinson,

* Corresponding author. Tel.: +1 302 831 0533; fax: +1 302 831 2281.
E-mail address: duncanm@udel.edu (M.K. Duncan).

0945-053X/$ – see front matter © 2009 Elsevier B.V. All rights reserved.
doi:10.1016/j.matbio.2009.12.004

1984; Comper et al., 1994; Russo et al., 2002), and it is difficult to assess the GBM's true contributions to glomerular permeability because of the presence of other sieving structures in the glomerular barrier (Haraldsson et al., 2008; Smithies, 2003; Farquhar, 2006).

While all molecules important for lens physiology must transit the capsule, the permeability parameters of the capsule have not been extensively studied. Unlike the GBM, the thickness and accessibility of the lens capsule make it an ideal basement membrane to study the mechanisms controlling selective permeability. However, early lens capsule permeability studies were typically performed using simple two-chambered systems which required whole lenses or lens capsules from large animals and were vulnerable to artifact due to the extensive tissue manipulation required to place the lens or capsule between the chambers (Fels, 1970; Fisher, 1977; Friedenwald, 1930a; Delamere and Duncan, 1979; Ozaki, 1984; Kinsey and Reddy, 1965; Lee et al., 2006; Fisher, 1982; Takeguchi and Nakagaki, 1969). These experiments only measured the diffusivity of water, small charged tracer molecules, or polysaccharides, not biologically significant proteins. Other studies measured the uptake of tracking molecules or proteins into whole lenses and attempted to draw qualitative conclusions about lens permeability (Boyle et al., 2002; Sabah et al., 2004; Yan et al., 2002); but this technique makes it very difficult to distinguish between the permeability of the capsule and that of the cellular membranes.

In this study, we report a novel approach towards describing lens capsule permeability using fluorescence recovery after photobleaching (FRAP). This approach allows the quantitative determination of the lens capsule's permeability to biologically significant proteins and the matrix binding affinities of these proteins to the capsules of living lenses. Because of its relative thickness and good accessibility, the lens capsule, unlike the GBM, serves as an ideal model system for studying the transport mechanisms underlying selective permeability of basement membranes. Our results on mouse lens capsules show an interesting dichotomy between the permeability and binding of proteins endogenous to the lens environment versus dextrans within lens capsule matrices. We also performed a series of protein diffusion experiments involving lens capsules with modified anionic and cationic sites as well as blocked hydrophobic interactions. Our results revealed a complex mechanism responsible for the selective permeability of the lens capsule, a mechanism based on a molecule's size and shape as well as ionic and hydrophobic interactions.

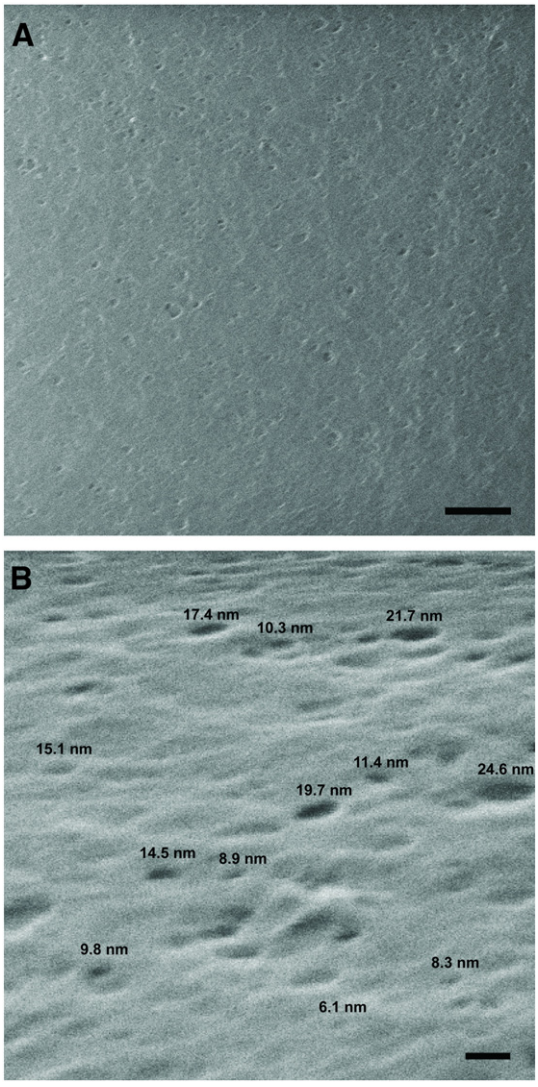

Fig. 1. Helium ion microscopy of the anterior lens capsule of an adult mouse lens A) Top–down view of the anterior capsule, bar = 200 nm. B) Surface image acquired at a 40 ° tilt. Representative diameters are provided above selected pores, bar = 20 nm.

2. Results

2.1. Permeability of the lens capsule

All molecules entering the avascular lens must transit the lens capsule prior to reaching the lens cells. The capsule is composed of a matrix of basement membrane molecules which create a series of intertwining pores through its entire thickness. Permeability through the capsule has been proposed to be influenced by its effective pore size and charged domains (Friedenwald, 1930b). The surface of the lens capsule visualized by scanning helium ion microscopy shows the surface of the capsule interspersed with openings ranging in size from approximately 25 nm to 6 nm (Fig. 1A, B). In order to determine how efficiently molecules of different Stokes radii (R_S) would enter the capsule, the partition coefficients (Φ) of five polydisperse fluorescein labeled dextrans (highly branched and flexible polysaccharides), with nominal molecular weights of 3 kDa, 10 kDa, 40 kDa, 150 kDa and 250 kDa, and seven fluorescein labeled proteins which are endogenous to the lens environment, EGF, γD-crystallin, a naturally occurring, cataract-associated mutant form of γD-crystallin [E107A] (Messina-Baas et al., 2006), BSA, transferrin, ceruloplasmin, and IgG were determined using confocal microscopy. The physical properties of all tracers used in the study are listed in supplemental Table 1. The partition coefficients measured for the 3–150 kDa dextrans decreased inversely to their Stokes radii (R_S), 0.74, 0.42, 0.27, and 0.25 (Fig. 2A). The partition coefficient for the 250 kDa dextran was 0.32, which was slightly higher than the value for the 150 kDa dextran; possibly a result of the capsule matrix excluding the larger molecules of its polydispersed range (average R_S of 10.9 nm). Partition coefficients for the smaller proteins, EGF, WT and mutant γD-crystallin were 2.54, 2.74, and 2.49, respectively, more than 3.5 times higher than the 3 kDa and 10 kDa dextrans (Fig. 2A). Interestingly, a single amino acid substitution of a negative glutamic acid with a neutral alanine [E107A] resulted in a 9.1% decrease in Φ for γD-crystallin. The four larger proteins, transferrin, BSA, ceruloplasmin, and IgG, each had Φ values closer to those measured for the 40 kDa dextran, 0.32, 0.29, 0.68, and 0.31, respectively (Fig. 2A). Experiments were also performed using fluorescein labeled IGF and insulin, however Φ could not be determined due to intramolecular fluorescence quenching (Lakowicz, 2006) within the lens capsule. Values and standard errors experimentally determined in unmodified capsules can be found in supplemental Table 1.

Molecules diffusing within the lens capsule are hindered compared with free diffusion in aqueous solution, due to various physical and chemical interactions with the surrounding extracellular matrix. We describe this hindered diffusion with three parameters, the effective diffusion coefficient (D) in the lens capsule, the relative

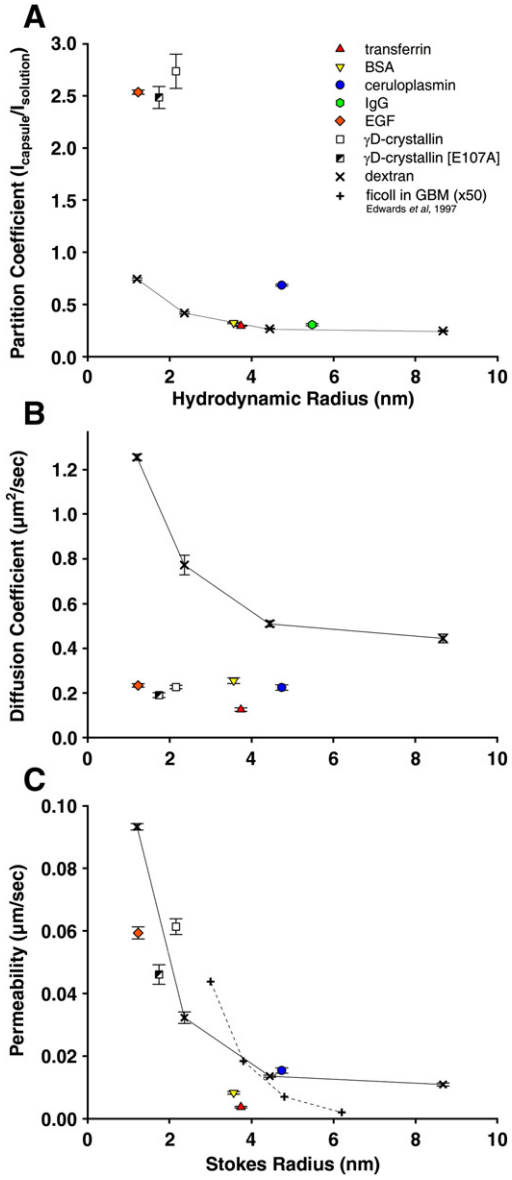

Fig. 2. Behavior of fluorescein labeled dextrans and protein in the anterior mouse lens capsule as a function of Stoke's radius. A) The equilibrium partition coefficient of these molecules calculated by dividing the fluorescence intensity within the capsule ($I_{capsule}$) by the fluorescent intensity in solution ($I_{solution}$). B) The diffusion coefficients for the studied molecules within the capsule evaluated from FRAP recovery curves. C) The calculated permeability of dextrans and proteins in the lens capsule. These values are compared to permeability values determined for Ficoll in the glomerular basement membrane (adjusted for thickness) determined by Edwards et al. (2007).

diffusivity ($D_{\text{lens capsule}}/D_{\text{solution}}$), and the binding affinity ratio of the molecules to the capsule matrix ($k_{\text{dissociation}}/k_{\text{association}}$).

The dextrans diffused at rates inverse to their R_S, 1.26, 0.77, 0.51, and 0.45 μm^2/s (Fig. 2B) which was comparable to, but slightly slower, than the diffusion rates previously measured in the lens capsule for similarly sized dextrans using a two-chambered system (Lee et al., 2006). Relative diffusivity is a useful comparison of the diffusion of a molecule in the capsule versus in solution. Interestingly, the relative diffusivity ($D_{\text{lens capsule capsule}}/D_{\text{solution}}$) of the dextrans increased with their size, 0.74%, 0.89%, and 1.10%, and 1.87%. Overall, protein diffusion in the capsule was appreciably slower than for dextrans of similar sizes. Diffusion coefficients in the capsule for EGF, γD-crystallin, γD-crystallin [E107A], BSA, transferrin, and ceruloplasmin, were 0.23, 0.17, 0.18, 0.26, 0.13, and 0.22 μm^2/s, respectively (Fig. 2B). In contrast, IgG did not diffuse sufficiently within the capsule during the time frame of the experiment (50 seconds) to provide adequate recovery curves. The relative diffusivity of proteins in the capsule was also lower than the values for dextrans, 0.14%, 0.23%, 0.15%, 0.44%, 0.23%, and 0.52%, for EGF, γD-crystallin, γD-crystallin [E107A], BSA, transferrin, and ceruloplasmin, respectively.

The permeability (P) of the lens capsule to dextrans decreased inversely to their average R_S and molecular weight, 0.09, 0.03, 0.01, and 0.01 μm/s, for the 3 kDa, 10 kDa, 40 kDa, and 150 kDa respectively. These values are comparable to the published permeability of the GBM (adjusted for thickness) to similar sized dextrans (Edwards et al., 1997) (Fig. 2C). Although the proteins were able to enter the capsule at higher equilibrium concentrations than dextrans (i.e., higher Φ), they diffused at slower rates (i.e., lower D). Therefore, some protein permeability values were in line with the values calculated for dextrans of similar R_S. The lens capsule permeability values for γD-crystallin, γD-crystallin [E107A], and ceruloplasmin were, 0.061, 0.046, and 0.015 μm/s, respectively, which were similar to that of comparably sized dextrans. EGF, BSA, and transferrin had markedly lower permeability values than those of similarly sized dextrans, 0.059, 0.008, and 0.004 μm/s, respectively (Fig. 2C).

2.2. Molecule binding in the lens capsule

Some proteins, especially growth factors, are known to bind to core basement membrane proteins and heparan sulfate side chains (Chu et al., 2005; Kreuger et al., 2005; Lamanna et al., 2007; Uchimura et al., 2006). Proteins participating in low affinity binding can be described using the ratio of the kinetic dissociation and association constants (k_d/k_a) which we will term as the binding affinity ratio. We also report the immobile fraction of the studied tracers from FRAP recovery curves. The immobile fraction is the unrecovered fluorescence intensity within the lens capsule after bleaching a circular region of interest (ROI) and represents bleached and unbleached fluorescein labeled molecules unable to exchange in the X–Y plane during the time frame of the experiment (Axelrod et al., 1976).

Binding strength of the tested molecules to the lens ECM varied greatly. It would be expected that a neutral polysaccharide, such as a dextran molecule, would have little binding affinity towards the capsule. This was observed for the smaller dextrans, 3 kDa, 10 kDa, and 40 kDa, each having immobile fractions of less than 5% at the completion of the experiment (17 s duration). However, close to 30% of the larger 150 kDa dextran was unable to diffuse out of the ROI (Fig. 3A). Proteins bound to the capsule matrix much more tightly than dextrans, with immobile fractions 5 to 50 times greater than dextrans of similar R_S (50 s duration). EGF, γD-crystallin, γD-crystallin [E107A], BSA, transferrin, ceruloplasmin, and IgG had immobile fractions of 29.6%, 74.2%, 55.0%, 70.9%, 49.2%, 54.9%, and 93.2%, respectively (Fig. 3A). Protein binding affinity ratios, where lower values indicate stronger binding, were at least five times lower compared to dextrans of similar R_S. Binding affinity ratios for the 3 kDa, 10 kDa, 40 kDa, and 150 kDa dextrans were 17.6, 6.5, 2.8, and 1.9, respectively. Whereas binding affinity ratios for EGF, γD-crystallin, γD-crystallin [E107A], BSA, transferrin, and ceruloplasmin were 4.65, 0.45, 0.92, 0.49, 1.59, and 0.92, respectively (Fig. 3B).

2.3. Anionic interactions between proteins and the lens capsule

We have demonstrated that proteins diffuse and interact within the lens capsule in a fashion appreciably different from polysaccharides. Next we attempted to investigate how ionic and hydrophobic interactions influence protein behavior in the capsule. It is believed that size and ionic interactions between proteins and basement membranes molecules are the main determinant of protein permeability in the GBM (Kanwar et al., 1980; Bertolatus and Hunsicker, 1987; Bridges et al., 1991; Morita et al., 2005); but this has only been explored in the lens capsule using relatively small charged tracer

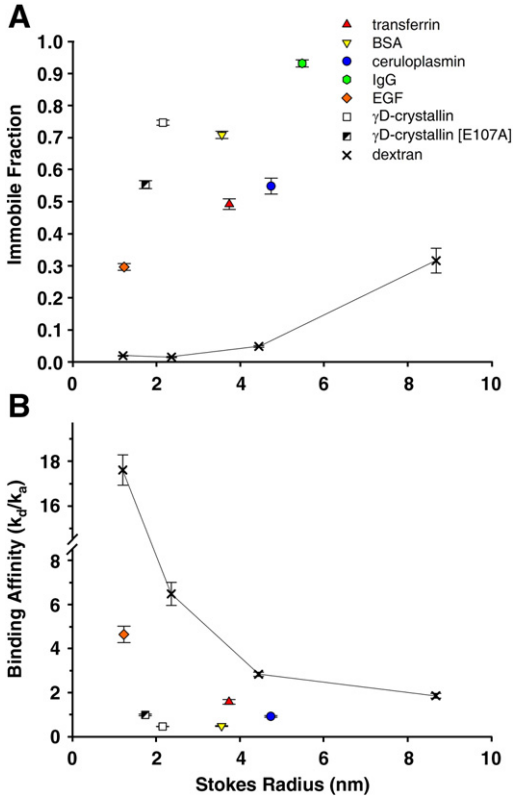

Fig. 3. Lens capsule matrix interactions of fluorescein labeled dextrans and proteins. A) Comparison of the immobile fractions of each molecule and B) their binding affinity ratios evaluated from FRAP recovery curves.

molecules (Friedenwald, 1930b). We investigated the influence of ionic interactions on lens capsule permeability and binding by targeting two sources of anionic charges within the lens capsule, carboxyl groups and heparan sulfate side chains, as well as a source of cationic charge, amine groups (described in the next section). Partition coefficients (Φ) increased for all proteins tested in lens capsules following the irreversible capping of carboxyl groups with glycine methyl ester. The Φ of EGF, γD-crystallin, BSA, transferrin, ceruloplasmin, and IgG, significantly increased by 71.8%, 31.3%, 46.1%, 25.6%, 97.3%, and 28.1%, respectively, whereas the change for γD-crystallin [E107A] was not statistically significant compared to measurements in unmodified capsules (Fig. 4A). In heparanase treated lens capsules, there were also significant increases in Φ for transferrin, BSA, and IgG, 23.2%, 17.4%, 13.0%, respectively; however, Φ for ceruloplasmin and EGF did not significantly change with heparanase treatment (Fig. 4A). Partition coefficient percent changes, standard errors, and p values for proteins in modified capsules can be found in supplemental Table 2.

The diffusion coefficient did not change universally as was observed for Φ in lens capsules with neutralized anionic sites. When carboxyl groups were blocked, BSA diffused significantly faster, 76.3%, whereas, transferrin, EGF, and γD-crystallin diffused significantly slower, −32.5%, −38.7%, −54.5%, respectively. Ceruloplasmin and γD-crystallin [E107A] did not significantly change when compared to values in unmodified capsules (Fig. 4B). In heparanase treated capsules, only transferrin significantly slowed by −35.2%, while D did not significantly change for BSA, ceruloplasmin, γD-crystallin, γD-crystallin [E107A], or EGF (Fig. 4B).

Changes in permeability values calculated for proteins in lens capsules with modified anionic sites varied. In capsules with blocked carboxyl groups, the permeability of BSA and ceruloplasmin both significantly increased, 157.7% and 86.7%, while γD-crystallin signif-

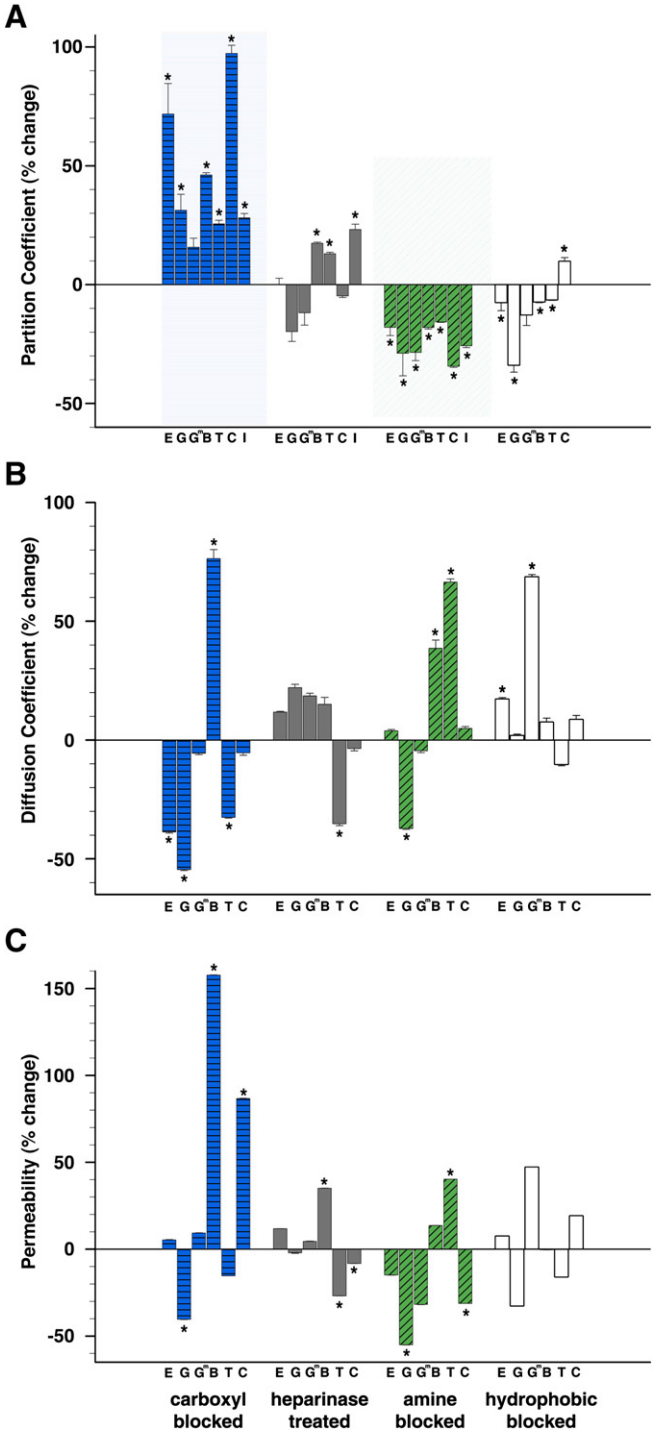

Fig. 4. Change in protein behavior in mouse anterior capsules modified by neutralizing carboxyl or amine groups, removal of heparan sulfate side chains, or blocking hydrophobic interactions. Proteins are listed from smallest to largest. A) Percent change of partition coefficients from values determined in unmodified capsules. B) Percent change of diffusion coefficients from values determined in unmodified capsules. C) Percent change of permeability values from values determined in unmodified capsules. (E = EGF, G = γD-crystallin, G^m = γD-crystallin [E107A], B = BSA, T = transferrin, C = ceruloplasmin, and I = IgG) (*p<=0.05).

icantly decreased by −40.3%; EGF, γD-crystallin [E107A], and transferrin did not significantly change (Fig. 4C). Permeability significantly changed for BSA, transferrin, and ceruloplasmin, 35.1%, −26.8%, and −8.1%, respectively, in lens capsules with cleaved heparan sulfate side chains, but did not change significantly for EGF, γD-crystallin, or γD-crystallin [E107A] (Fig. 4C).

Neutralizing or removing anionic sites within the lens capsule also strengthened protein–matrix interactions. Significant increases in matrix binding were observed in these capsules for many of the proteins tested, demonstrated by significant increases in immobile fractions and decreases in binding affinity ratios. The immobile fractions of EGF, γD-crystallin, BSA, transferrin, and ceruloplasmin increased in capsules with neutralized carboxyl groups by 96.5%, 10.7%, 24.8%, 61.3%, and 57.3%, respectively (Fig. 5A) while the immobile fractions of γD-crystallin [E107A] and IgG did not significantly change. Additionally, in these capsules, the binding affinity ratios for EGF, BSA, transferrin, and ceruloplasmin significantly decreased, −66.2%, −60.2%, −70.7%, and −63.3%, respectively, whereas γD-crystallin and γD-crystallin [E107A] did not significantly change (Fig. 5B). In heparanase treated capsules, the immobile fractions of BSA and transferrin increased, 10.7% and 57.3%, while γD-crystallin and γD-crystallin [E107A] significantly decreased, −28.0% and −46.8% (Fig. 5A). EGF, ceruloplasmin, and IgG did not significantly change. Similarly, significant decreases in binding affinity ratios in these capsules were observed for BSA and transferrin, −26.6% and −69.1%, and showed a decrease in binding of γD-crystallin and γD-crystallin [E107A] to the capsule, where the binding affinity ratio increased 136.1% and 58.4% (Fig. 5B). No significant changes were measured for EGF and ceruloplasmin.

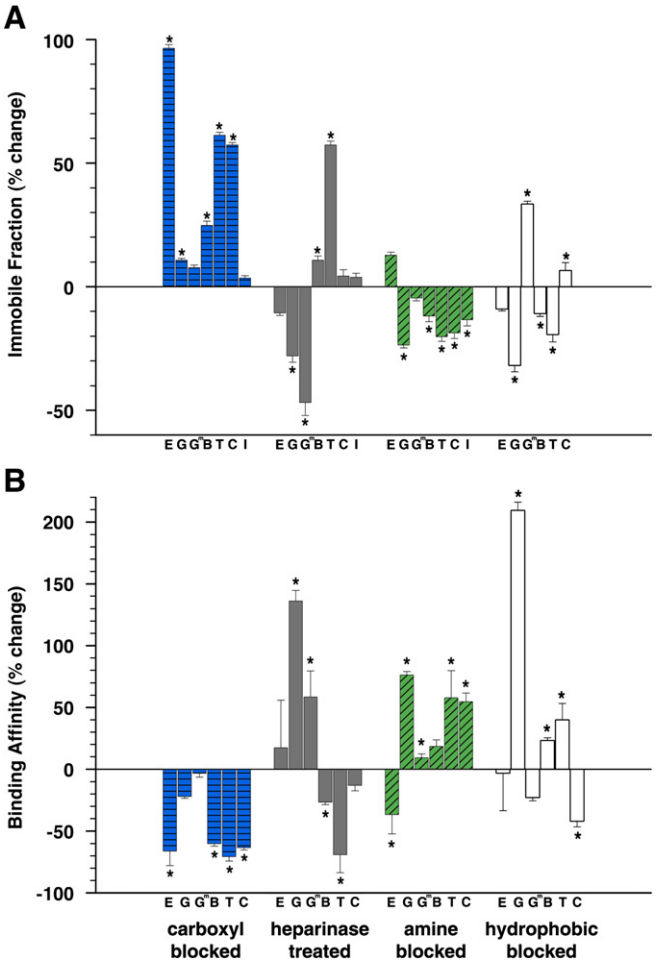

Fig. 5. Change in matrix interactions in modified lens capsules. A) Percent change of immobile fractions of proteins from values determined in unmodified capsules. B) Change in binding affinity ratios. (E = EGF, G = γD-crystallin, G^m = γD-crystallin [E107A], B = BSA, T = transferrin, C = ceruloplasmin, and I = IgG) (*p<=0.05).

2.4. Cationic interactions between proteins and the lens capsule

Partition coefficients, diffusivity, permeability, and matrix binding were also tested in lens capsules in which cationic amine groups were irreversibly capped and neutralized with sulfo-NHS acetate. In contrast to removing anionic sites, neutralizing cationic sites in the capsule decreased Φ values of all proteins tested. EGF, γD-crystallin, γD-crystallin [E107A], BSA, transferrin, ceruloplasmin, and IgG significantly decreased compared to values in untreated capsules, −118.0%, −28.8%, −28.5%, −18.0%, −15.7%, −34.4%, and −25.7%, respectively (Fig. 4A). In these capsules, the diffusion coefficients of BSA and transferrin significantly increased, 38.6% and 66.4%; whereas, the diffusion speed of γD-crystallin significantly decreased, −37.2%, while γD-crystallin [E107A], EGF and ceruloplasmin did not significantly change (Fig. 4B). Although the effects of a more negatively charged capsule on the Φ of the proteins were consistent, permeability varied. Permeability for γD-crystallin and ceruloplasmin significantly decreased by −55.0% and −31.2%, while transferrin significantly increased by 40.3% (Fig. 4C). EGF, γD-crystallin [E107A], and BSA did not significantly change.

Changes in immobile fraction and binding affinity ratios in capsules with neutralized amine groups demonstrated a decrease in matrix binding for most of the proteins. The immobile fractions of γD-crystallin, BSA, transferrin, ceruloplasmin, and IgG decreased by −23.6%, −11.8%, −20.2%, −18.7%, and −13.4%, respectively. EGF and γD-crystallin [E107A] did not significantly change (Fig. 5A). Binding affinity ratios significantly increased for γD-crystallin, transferrin, and ceruloplasmin, 76.3%, 57.9%, and 54.7%, respectively (Fig. 5B). Conversely, binding affinity ratios significantly decreased by −36.7% for EGF, describing stronger matrix binding in more anionic capsules. No significant change in the binding affinity ratios of γD-crystallin [E107A] and BSA were observed.

2.5. Hydrophobic interactions within the lens capsule

Soluble proteins fold into tertiary structures which hide their hydrophobic regions. However, some hydrophobic regions still remain exposed on their surfaces. We investigated the influence of hydrophobic interactions on lens capsule permeability and matrix binding by performing FRAP experiments in the presence of the mild non-ionic surfactant octyl-β-D-glucopyranoside. Partition coefficients significantly decreased for EGF, γD-crystallin, γD-crystallin [E107A], BSA, and transferrin, −7.5%, −33.8%, 12.7%, −7.2%, and −6.4%, respectively, and significantly increased by 9.8% for ceruloplasmin (Fig. 4A). The rate of diffusion significantly increased by 17.2% for EGF and 68.6% for γD-crystallin [E107A], but did not significantly change for γD-crystallin, BSA, transferrin, or ceruloplasmin (Fig. 4B). Overall though, permeability did not significantly change for any of the proteins tested in capsules with blocked hydrophobic interactions (Fig. 4C).

For most of the proteins, blocking hydrophobic interactions with the capsule matrix altered binding. Matrix binding for BSA and transferrin decreased, as their immobile fractions decreased by −10.8% and −19.3%, and their binding affinity ratios increased by 23.2% and 39.8%, both respectively. Conversely, matrix binding increased for ceruloplasmin, with a significant increase in the immobile fraction, 6.5%, and a significant decrease in the binding affinity ratio, −41.9% (Fig. 5A, B). Interestingly, substituting a single hydrophilic glutamic acid on the surface of γD-crystallin with the more hydrophobic alanine resulted in opposing changes to matrix binding in this environment (Fig. 5A, B). Binding of γD-crystallin to the capsule matrix decreased when hydrophobic interactions were blocked, with a significant decrease, −31.8%, in immobile fraction and a significant increase, 209.3%, in its matrix binding affinity ratio, whereas binding increased for mutant γD-crystallin [E107A], with a 33.4% increase in the immobile fraction. Capsule matrix binding did not significantly change for EGF.

3. Discussion

In the present investigation we performed a series of experiments utilizing an *in situ* approach based on FRAP to fully characterize the diffusive behavior of not only polysaccharides but also proteins endogenous to the lens capsule environment and important for lens and eye health. For instance, crystallins leaking from lens fiber cells through intact capsules can cause severe eye inflammation (Denis et al., 2003). EGF, IGF, and insulin are vital for proper lens cell growth and differentiation (Lovicu and McAvoy, 2005), while the carrier proteins BSA, transferrin, and ceruloplasmin are responsible for the endo- and transcytotic delivery of the iron, copper, and fatty acids essential for normal cell metabolism to the lens (Sabah et al., 2005, 2007; Harned et al., 2006). The FRAP method is relatively quick and non-invasive compared to the previous transport chamber method that required extensive tissue manipulation and limited their descriptions to only the sieving or diffusion coefficients of polysaccharides or water (Fels, 1970; Fisher, 1977; Friedenwald, 1930a; Delamere and Duncan, 1979; Ozaki, 1984; Kinsey and Reddy, 1965; Lee et al., 2006; Fisher, 1982; Takeguchi and Nakagaki, 1969). Furthermore, we modified ionic and hydrophobic sites in the capsule matrix in order to examine their influence on solute diffusion, which has been long speculated, but was lacking in experimental evidence.

The overall permeability of these molecules through the lens capsule appeared to be inversely related to the solute size (Fig. 2C); suggesting that steric exclusion between solutes and matrix pores had a strong influence on permeability. Helium ion microscopy of a native mouse lens showed openings on the surface of the capsule with a maximum diameter near 25 nm. However, its effective pore size may be smaller due to the overlay of pores at different layers throughout the thickness (10 μm) of the mouse lens capsule (Danysh et al., 2008). In fact the effective pore size may be closer to the maximum pore diameter of 20 nm which some have predicted for the GBM (Tencer et al., 1998; Venturoli and Rippe, 2005). Notably, experimental evidence of our predicted maximum capsule pore size is in our observation that the polydisperse 250 kDa dextrans (with an average R_S of 10.9 nm and we estimate to have a range of 10.5–12.0 nm) had limited access to the capsule matrix. This limited access we presume is a result of only the smaller molecules of the population being capable of entering the matrix pores. In other studies, larger objects (2000 kDa dextrans, $R_S = \sim 27$ nm; and type-5 adenovirus vectors, $R_S = \sim 49$ nm) were shown to pass through the lens capsule in a two-chamber diffusion system (Chua and Perks, 1998) or after anterior chamber injection (Curiel and Douglas, 2002; Robertson et al., 2007). Considering the maximum pore size we have measured in the capsule, this contradiction may suggest that the capsules used in the previous reports were compromised.

The relative diffusivity of both larger dextrans and proteins within the capsule was somewhat higher than for smaller molecules. This suggested that the lens capsule had heterogeneous pores similar to beads in a size exclusion column. In both, smaller molecules were slowed by entering smaller pores, while larger molecules were excluded and diffuse more rapidly (Mori and Barth, 1999).

In addition to the steric influence the capsule matrix has on solute diffusion, our data also suggested that ionic and hydrophobic interactions had a significant influence on lens capsule permeability and matrix binding. The current dogma presumes that the repulsive interactions between anionic sites on protein surfaces and the membrane matrix is the major force controlling basement membrane permeability. While it was not possible to quantitate how completely our treatments removed all charged groups from the capsule due to the presence of attached lens cells, our data show reducing the number of anionic sites in the capsule resulted in an almost universal increase in matrix binding and protein equilibrium concentrations. Conversely, cationic sites in the capsule appeared to attract proteins since reducing their number decreased matrix binding and equilibrium concentrations of most proteins. While it is possible that neutralization of carboxyl and amine groups or the removal of heparan sulfate side chains affect the structure and size of the capsule matrix pores, the lack of correlation between the equilibrium concentration and diffusion rates of proteins within modified capsules with the protein's size makes this interpretation unlikely. It could then be presumed that the removal of an anionic patch from the surface of a protein would result in an increase in matrix binding. For the mutant γD-crystallin, the substitution of a glutamic acid for an alanine [E107A] removes an anionic patch on the protein's surface, increasing its measured isoelectric point from 7.3 to 8.3 without altering its structure (Pande et al., 2009). However, γD-crystallin [E107A] had a significantly lower immobile fraction ($p = 0.004$) and a significantly higher binding affinity ratio ($p<0.001$) in the capsule matrix compared to γD-crystallin. This indicates that the attractive forces between anionic sites on protein surfaces and the cationic sites in a membrane matrix may have more of an influence on protein behavior within basement membranes than was previously expected. In this context, the increase in binding and partition coefficients for proteins in lens capsules with neutralized carboxyl groups can conceivably be explained as an increase in cationic sites in the membrane matrix as a result of broken salt bridges.

Undoubtedly ionic interactions between proteins and the lens capsule matrix influence the behavior of proteins diffusing within a basement membrane. However, protein behavior in the capsule cannot be easily predicted based on estimated isoelectric points (MathWorks, 2008). Diffusion rates in unmodified capsules and rate changes in charge modified capsules do not correlate to a protein's isoelectric point. Additionally, in many experiments performed in modified capsules the behavior of γD-crystallin [E107A] did not significantly change where γD-crystallin did. This suggested that a single anionic patch on the surface of a protein has a substantial influence on its ability to enter and diffuse within the lens capsule.

Our results demonstrated that molecules with charged surface regions behave very differently than uncharged polysaccharides in the capsule. Although we saw substantial differences in equilibrium concentrations and diffusion rates between dextrans and proteins, their permeability values were similar since slower protein diffusion negates the increased protein equilibrium concentrations. Despite this, capsule permeability still seemed to be influenced by charged sites within the capsule matrix.

4. Experimental procedures

4.1. Molecule labeling and purification

The 3 kDa, 10 kDa, and 40 kDa dextrans (Invitrogen, Carlsbad, CA), 150 kDa and 250 kDa dextrans (Sigma-Aldrich, St. Louis, MO), BSA (#A23015, Invitrogen, Carlsbad, CA), EGF (#E3478, Invitrogen, Carlsbad, CA), holo-transferrin (#T2871, Invitrogen, Carlsbad, CA), and rabbit anti-goat IgG (#A10529, Invitrogen, Carlsbad, CA) were purchased as fluorescein conjugates. Ceruloplasmin (#C2026, Sigma-Aldrich, St Louis, MO), IGF (#4119-1000, BioVision, Mountain View, CA), recombinant wild type γD-crystallin and mutant γD-crystallin [E107A] (Pande et al., 2009, 2000) were labeled using the following protocol. Proteins (10–20 mg/ml) were dialyzed into 0.1 M sodium bicarbonate buffer. Fluorescein succinimidyl ester (#C1311, Invitrogen, Carlsbad, CA) (10 mg/ml) was dissolved in DMSO and 100 μl was added to the sodium bicarbonate buffer containing the protein then incubated at room temperature for 1 hour. Unreacted fluorescein was then removed using an 18 ml G25 Sephadex™ column. The concentration of fluorescein labeled molecules used in the experiments was approximately 1.0 mg/ml, except for EGF which was used at 0.1 mg/ml. This is compared to the total protein concentration of 0.3 to 0.7 mg/ml reported in human and rabbit aqueous humors (Duan et al., 2008; Funding et al., 2005; Liu et al., 1998).

4.2. Mouse lens preparations

Lenses for were isolated from 8–12 week old FVB/N mice and gently rolled on paper toweling to remove extralenticular tissue. The lenses were then washed with PBS (pH 7.4) on an orbital rocker for 30–45 minutes at 90 revolutions per minute (rpm).

Carboxyl groups were capped and neutralized with glycine methyl ester (GME, #G6600, Sigma-Aldrich, St Louis, MO) using the cross-linking activator 1-ethyl-3-[3-dimethylaminopropyl] carbodiimide hydrochloride (EDC, #26777, ThermoFisher Scientific, Waltham, MA). Whole lenses were placed in PBS containing 0.01 M GME and 0.1 M EDC then incubated for 1 hour at room temperature, then washed in PBS for 30–45 min (Bertolatus and Klinzman, 1991).

Amine groups were capped and neutralized with sulfo-NHS acetate (#26777, Pierce, Rockford, IL). Whole lenses were placed in PBS containing sulfo-NHS acetate (6.25 mg/ml) and incubated for 1 hour at room temperature, then washed in PBS on an orbital rocker for 30–45 minutes at 90 rpm.

Heparan sulfate side chains were enzymatically cleaved using heparanase II (#H6512, Sigma-Aldrich, St Louis, MO) which cleaves heparan sulfate at both glucuronic and iduronic acid residues (Linhardt et al., 1990). Whole lenses were placed in 500 µl of PBS containing 40 mIU heparanase II and incubated at 30 °C for 4 hours. Lenses were then washed in PBS on an orbital rocker for 30–45 minutes at 90 rpm (Bertolatus and Klinzman, 1991).

Hydrophobic interactions were blocked using the mild non-ionic surfactant octyl-β-D-glucopyranoside (#O8001, Sigma-Aldrich, St Louis, MO). Whole lenses were placed in a PBS solution containing 10 mM of octyl-β-D-glucopyranoside (less than half its critical micelle concentration) (Konidala et al., 2006) for 30 minutes at room temperature prior to each experiment. Loading and FRAP experiments were then carried out in fresh surfactant solution containing the labeled proteins.

Although the precise efficiency of each treatment was not accessed through empirical methods, their effectiveness can be observed in changes in the partition coefficients of the proteins. The effectiveness of heparanase II was most likely limited by steric hindrance of the 84 kDa molecule within the lens capsule matrix.

To assist with lens orientation, epithelial cell nuclei were treated with the vital nuclear stain DRAQ-5™ (0.5 µl/ml) (#DR500, Biostatus Ltd., Leicestershore, UK) for a minimum of 20 minutes at room temperature.

4.3. Partition coefficients and fluorescence recovery after photobleaching (FRAP)

Whole lenses of wild type FVB/N mice (8–12 week old) were placed in #1.5 cover slip dishes containing the solution of fluorescein labeled dextran or protein of interest in PBS. Labeled molecules were allowed to equilibrate into lens capsules for at least 10 minutes prior to partition coefficient and FRAP experiments. Longer incubation periods did not affect results for molecules described in this study. Fluorescence intensity data for both FRAP and partition coefficient experiments were obtained from images acquired using a 40× C-Apochromat water immersion objective (NA = 1.2) on a Zeiss AxioObserver Z1 inverted microscope configured as an LSM 5DUO confocal (with both LSM510 META and LSM5 LIVE scanheads).

Partition coefficients were determined using the fluorescence intensity data from *X*–*Y* plane confocal images of the anterior lens capsule at a distance of 50 µm from the cover slip. The fluorescence intensity ratio averaged from 50 consecutive points from within the middle of the capsule and 50 consecutive points from the surrounding media was used to determine a partition coefficient.

FRAP experiments were performed along the *X*–*Y* plane within the anterior lens capsule at a depth of 6 µm. A 2.5 µm radius circular region of interest (ROI) was chosen at random in the center of the anterior capsule and average fluorescence intensity data was acquired from confocal images at a rate of 20 fps. A 100 mW 488 diode laser was directed from the META scanhead via an 80/20 mirror to bleach the ROI, while all image acquisition utilized the 5LIVE scanhead with a 495 long pass emission filter. Ten pre-bleach images were acquired prior to bleaching the ROI for 50 ms (100% laser power) followed by 350 or 1000 post-bleach images for dextran and protein experiments, respectively. The number of images taken after photobleaching the ROI was determined as the effective completion of fluorescence recovery and allowed comparable immobile fraction results for each type of molecule, dextrans and proteins. Each series of FRAP experiments were performed on three or four lenses using five or six different ROIs from each lens.

4.4. Recovery curve fitting and variable evaluation

A diffusion-reaction model was developed to describe tracer concentration after photobleaching in an infinite homogenous domain. In this model, the fractions that bind to the lens ECM (immobile) and that freely diffuse in the aqueous solution within the porous lens ECM (mobile) are explicitly considered. The binding and dissociation between the two states are assumed to follow first-order reaction kinetics with linear association rate constants (k_d and k_a). A third reaction term k_b is added to describe the loss of fluorescence for both immobile and mobile fractions due to inherent bleaching of the fluorescent signal during the post-bleach image acquisition. The spatiotemporal distribution of the fluorescence in the studied domain is thus described as the following equations:

$$\frac{\partial F^m}{\partial t} = (D\nabla^2 F^m) + (k_d F^i - k_a F^m) - k_b F^m \tag{1a}$$

$$\frac{\partial F^i}{\partial t} = (k_a F^m - k_d F^i) - k_b F^i \tag{1b}$$

where t is time immediately after photobleaching; F^m and F^i are the fluorescence intensities from mobile and immobile molecules, respectively; D is the diffusion coefficient of the mobile fraction; k_d and k_a are the kinetic dissociation and association rate constants; and k_b is the rate of autofading during continuous recording. The coupled Eq. (1a and b) were analytically solved using the following initial and boundary conditions: i) the photobleached circular spot where intensity is lowered by a factor of κ is created instantaneously at time 0 under 100% laser power; ii) the concentrations at the infinite boundary remain constant.

The detailed derivation of the analytical solution can be found in the document "Characterizing Molecular Diffusion in the Lens Capsule" from the 23rd Annual Workshop on Mathematical Problems in Industry, June 11–15, 2007, University of Delaware, Newark, DE (Edwards et al., 2007). A Matlab script was created to run iterative curve fittings. The function fminsearch provided in the Matlab toolbox was used to identify the free parameters (D, k_d, k_a, and k_b) that best fit the predicted fluorescence intensities in the experimental recordings. The goodness of the fitting was examined by the root-mean-square deviation. The initial estimate values were arbitrarily set to be $D = 1\ \mu m^2/s$; $k_d/k_a = 0.01$; $k_a = 0.1$; and k_b was chosen to be the exponential decay of the pre-bleach recording. Our analysis found that the final optimized parameters were not sensitive to the initial values and they always converged to the optimized values regardless of the initial estimate.

4.5. Determining permeability

From a molecule's partition and diffusion coefficients, the permeability (P) of the entire capsule to the molecule can be evaluated using (Edwards et al., 1997):

$$P = \frac{\phi D}{\delta} \tag{2}$$

where Φ is the molecule's partition coefficient; D is its diffusion coefficient within the capsule; and δ is the thickness of the capsule, approximately 10 μm for young FVB/N mice (Danysh et al., 2008). The physical meaning of the P indicates the amount of diffusive flux (J) of solute per unit surface area (A) of the lens capsule per unit concentration difference between inside and outside of the lens capsule (ΔC) (i.e., $J/A = P\Delta C$).

4.6. Determining diffusion coefficients and Stokes radii in solution

To determine diffusion coefficients in solution, FRAP experiments were performed on dextrans and proteins in PBS. Their half recovery times (time when half the initial photobleaching had recovered within the ROI) were determined using the kinetic analysis function in the Zeiss LSM AIM Software (Rel 4.2). The classic Axelrod model (Axelrod et al., 1976) was then used to calculate diffusion rates:

$$D = \frac{r^2 \gamma_D}{4\tau_{1/2}} \tag{3}$$

where r is the radius of the photobleached region of interest (ROI) which we established as 2.5 nm; γ_D is a factor accounting for the shape of the laser beam (0.88 for circular beams); $\tau_{1/2}$ is the half recovery time. A molecule's Stokes radius was then estimated using the Stokes–Einstein equation (Truskey et al., 2009):

$$R_h = \frac{k_B T}{6\pi n D_{\text{free}}} \tag{4}$$

where k_B is the Boltzmann constant ($1.38\times10^{-23} J\cdot K^{-1}$), T is room temperature (298 K), n is the viscosity of PBS assumed to be that of sea water ($1.06\times10^{-3}\,\text{kg}\cdot\text{m}^{-1}\,\text{s}^{-1}$), and D_{free} is the molecule's diffusion coefficient in PBS.

4.7. Statistical analysis

Statistical significance was determined using single factor analysis of variance (ANOVA), with $p<0.05$ indicating a significant difference. All error bars represent standard error.

4.8. Helium ion microscopy

Whole lenses were washed in 10 mM octyl-β-D-glucopyranoside for 60 minutes and then fixed in a 0.08 M sodium cacodylate buffer pH 7.4, 1.25% glutaraldehyde, 1% paraformaldehyde solution for about 2 hours. Fixed lenses were then washed in ddH2O (3×10 min) then placed in a 1% osmium tetroxide solution for 3 hours. The lenses were again washed in ddH2O (3×10 minutes) and then serially dehydrated in 25%, 50%, 75%, 80%, 95%, and 100% ethanol. Dehydrated lenses were then placed in a critical point drier for 3 hours and kept desiccated until imaged.

Helium ion microscopy (HIM) was performed on an Orion Plus (Carl Zeiss SMT). HIM is noted for its improved surface imaging compared to scanning electron microscopy and detailed theoretical and practical aspects of utilizing a helium ion source for imaging can be found in the literature (Morgan et al., 2006; Ward et al., 2006). No cleaning or coating was employed to the prepared lenses. Lenses were mounted with carbon conductive adhesive tabs to SEM stubs and HIM was carried out at a primary beam energy of 29.5 keV with a beam current of 0.3–0.4 pA. Secondary electron images were acquired with an off-axis Everhardt–Thornley detector. Top–down and tilted view (40 °) imaging was employed to facilitate visualization of the porous topology of the sample surface. Due to the insulating nature of our biological samples, a low energy (1 keV) electron flood beam was used to dissipate charge build-up during imaging. This process of charge neutralization was accomplished by multiplexing between the imaging operation and a diffuse electron flood pulse at the beginning of each scan line.

Acknowledgements

This work was supported by National Eye Institute Grant EY015279 to MKD, a Sigma-Xi/National Academy of Sciences research award and a GK-12 fellowship both awarded to BPD, a Beckman Young Scholars Fellowship to TPP, National Eye Institute grant EY010535 to JP, NIH COBRE program grant P20RR016459, NIAMS grant AR054385 and University of Delaware Research Foundation grants to LW. INBRE program grant P20 RR16472 supported the University of Delaware Bio-Imaging Center. The Authors would also like to thank Chuong Huynh, Larry Scipioni, and Arno Merkle (Carl Zeiss SMT, Inc., Peabody, MA) for their assistance with the helium ion microscopy.

Appendix A. Supplementary data

Supplementary data associated with this article can be found, in the online version, at doi:10.1016/j.matbio.2009.12.004.

References

Axelrod, D., Koppel, D.E., Schlessinger, J., Elson, E., Webb, W.W., 1976. Biophys. J. 16, 1055–1069.
Bertolatus, J.A., Hunsicker, L.G., 1987. Lab. Invest. 56, 170–179.
Bertolatus, J.A., Klinzman, D., 1991. Microvasc. Res. 41, 311–327.
Beyer, T.L., Vogler, G., Sharma, D., O'Donnell Jr., F.E., 1984. Invest. Ophthalmol. Vis. Sci. 25, 108–112.
Bray, J., Robinson, G.B., 1984. Kidney Int. 25, 527–533.
Bridges Jr., C.R., Rennke, H.G., Deen, W.M., Troy, J.L., Brenner, B.M., 1991. J. Am. Soc. Nephrol. 1, 1095–1108.
Boyle, D.L., Carman, P., Takemoto, L., 2002. Mol. Vis. 8, 226–234.
Cammarata, P., Cantu-Crouch, D., Oakford, L., Morrill, A., 1986. Tissue Cell 18, 83–97.
Chen, C.H., Hansma, H.G., 2000. J. Struct. Biol. 131, 44–55.
Chua, B.A., Perks, A.M., 1998. J. Physiol. 513 (Pt 1), 283–294.
Chu, C.L., Goerges, A.L., Nugent, M.A., 2005. Biochemistry 44, 12203–12213.
Comper, W.D., Tay, M., Wells, X., Dawes, J., 1994. Biochem. J. 297 (Pt 1), 31–34.
Cotlier, E., Fox, J., Bohigian, G., Beaty, C., Du Pree, A., 1968. Nature 217, 38–40.
Curiel, D., Douglas, J.T., 2002. Adenoviral Vectors for Gene Therapy. Academic Press, Amsterdam; Boston.
Danysh, B.P., Czymmek, K.J., Olurin, P.T., Sivak, J.G., Duncan, M.K., 2008. Anat. Rec. (Hoboken) 291, 1619–1627.
Danysh, B.P., Duncan, M.K., 2009. Exp. Eye Res. 88, 151–164.
Delamere, N.A., Duncan, G., 1979. J. Physiol. 295, 241–249.
Denis, H.M., Brooks, D.E., Alleman, A.R., Andrew, S.E., Plummer, C., 2003. Vet. Ophthalmol. 6, 321–327.
Duan, X., Lu, Q., Xue, P., Zhang, H., Dong, Z., Yang, F., Wang, N., 2008. Mol. Vis. 14, 370–377.
Edwards, A., Deen, W.M., Daniels, B.S., 1997. Biophys. J. 72, 204–213.
Edwards, D.A., Duncan, M.K., Danysh, B.P., Czymmek, K.J., Patel, T.P., Anthony, A., Breward, C., Gratton, M., Haider, M., Joshi, Y., Milgrom, T., Pelesko, J., Schleiniger, G., Ziao, Z., 2007. Characterizing molecular diffusion in the lens capsule. Twenty Third Annual Workshop on Mathematical Problems in Industry, University of Delaware, Newark, DE. http://www.math.udel.edu/~edwards/download/pubdir/pubo20.pdf.
Farquhar, M.G., 2006. J. Clin. Invest. 116, 2090–2093.
Fels, I.G., 1970. Exp. Eye Res. 10, 8–14.
Fisher, R.F., 1977. Trans. Ophthalmol. Soc. U.K. 97, 100–103.
Fisher, R.F., 1982. Proc. R. Soc. Lond. B Biol. Sci. 216, 475–496.
Friedenwald, J., 1930. Arch. Ophthalmol. 3, 182–193.
Friedenwald, J.S., 1930. Trans. Am. Ophthalmol. Soc. 28, 195–211.
Funding, M., Vorum, H., Honore, B., Nexo, E., Ehlers, N., 2005. Acta Ophthalmol. Scand. 83, 31–39.
Groffen, A.J., Ruegg, M.A., Dijkman, H., van de Velden, T.J., Buskens, C.A., van den Born, J., Assmann, K.J., Monnens, L.A., Veerkamp, J.H., van den Heuvel, L.P., 1998. J. Histochem. Cytochem. 46, 19–27.
Haraldsson, B., Nystrom, J., Deen, W.M., 2008. Physiol. Rev. 88, 451–487.
Harned, J., Fleisher, L.N., McGahan, M.C., 2006. Exp. Eye Res. 83, 721–727.
Konidala, P., He, L., Niemeyer, B., 2006. J. Mol. Graph Model 25, 77–86.
Karkinen-Jaaskelainen, M., Saxen, L., Vaheri, A., Leinikki, P., 1975. J. Exp. Med. 141, 1238–1248.
Kanwar, Y.S., Farquhar, M.G., 1979. J. Cell Biol. 81, 137–153.
Kanwar, Y.S., Farquhar, M.G., 1979. Proc. Natl. Acad. Sci. U.S.A. 76, 1303–1307.
Kanwar, Y.S., Linker, A., Farquhar, M.G., 1980. J. Cell Biol. 86, 688–693.
Kinsey, V.E., Reddy, D.V., 1965. Invest. Ophthalmol. 4, 104–116.
Krag, S., Andreassen, T.T., 2003. Prog. Retin. Eye Res. 22, 749–767.
Kreuger, J., Jemth, P., Sanders-Lindberg, E., Eliahu, L., Ron, D., Basilico, C., Salmivirta, M., Lindahl, U., 2005. Biochem. J. 389, 145–150.
Lakowicz, J.R., 2006. Principles of Fluorescence Spectroscopy3rd ed. Springer, New York.

Lamanna, W.C., Kalus, I., Padva, M., Baldwin, R.J., Merry, C.L., Dierks, T., 2007. J. Biotechnol. 129, 290–307.
Landemore, G., Stefani, P., Quillec, M., Lecoq-Guilbert, P., Billotte, C., Izard, J., 1999. Histochem. J. 31, 161–167.
Laurie, G.W., Bing, J.T., Kleinman, H.K., Hassell, J.R., Aumailley, M., Martin, G.R., Feldmann, R.J., 1986. J. Mol. Biol. 189, 205–216.
Lee, C.J., Vroom, J.A., Fishman, H.A., Bent, S.F., 2006. Biomaterials 27, 1670–1678.
Linhardt, R.J., Turnbull, J.E., Wang, H.M., Loganathan, D., Gallagher, J.T., 1990. Biochemistry 29, 2611–2617.
Liu, J.H., Lindsey, J.D., Weinreb, R.N., 1998. Invest. Ophthalmol. Vis. Sci. 39, 553–558.
Lovicu, F.J., McAvoy, J.W., 2005. Dev. Biol. 280, 1–14.
MathWorks, 2008. Matlab Bioinformatics Toolbox, v3.1 (R2008a). MathWorks Inc, Natick, MA.
Messina-Baas, O.M., Gonzalez-Huerta, L.M., Cuevas-Covarrubias, S.A., 2006. Mol. Vis. 12, 995–1000.
Mohan, P., Spiro, R., 1986. J. Biol. Chem. 261, 4328–4336.
Mori, S., Barth, H.G., 1999. Size Exclusion Chromatography. Springer, Berlin; New York.
Morita, H., Yoshimura, A., Inui, K., Ideura, T., Watanabe, H., Wang, L., Soininen, R., Tryggvason, K., 2005. J. Am. Soc. Nephrol. 16, 1703–1710.
Morgan, J., Notte, J.A., Hill, R., Ward, B.W., 2006. Microscopy Today 14, 24–31.
Ozaki, L., 1984. J. Am. Intraocul. Implant. Soc. 10, 182–184.
Pande, A., Banerjee, P.R., Patrosz, J., Pande, J., 2009. Invest. Ophthalmol. Vis. Sci. 50 E-abstract 1640.
Pande, A., Pande, J., Asherie, N., Lomakin, A., Ogun, O., King, J.A., Lubsen, N.H., Walton, D., Benedek, G.B., 2000. Proc. Natl. Acad. Sci. U. S. A. 97, 1993–1998.
Parthasarathy, N., Spiro, R.G., 1982. Arch. Biochem. Biophys. 213, 504–511.
Robertson, J.V., Nathu, Z., Najjar, A., Dwivedi, D., Gauldie, J., West-Mays, J.A., 2007. Mol. Vis. 13, 457–469.
Robinson, M.L., 2006. Semin. Cell Dev. Biol. 17, 726–740.
Rossi, M., Morita, H., Sormunen, R., Airenne, S., Kreivi, M., Wang, L., Fukai, N., Olsen, B., Tryggvason, K., Soininen, R., 2003. EMBO J. 22, 236–245.
Russo, L.M., Bakris, G.L., Comper, W.D., 2002. Am. J. Kidney Dis. 39, 899–919.
Sabah, J., McConkey, E., Welti, R., Albin, K., Takemoto, L.J., 2005. Exp. Eye Res. 80, 31–36.
Sabah, J.R., Davidson, H., McConkey, E.N., Takemoto, L., 2004. Mol. Vis. 10, 254–259.
Sabah, J.R., Schultz, B.D., Brown, Z.W., Nguyen, A.T., Reddan, J., Takemoto, L.J., 2007. Invest. Ophthalmol. Vis. Sci. 48, 1237–1244.
Smithies, O., 2003. Proc. Natl. Acad. Sci. U.S.A. 100, 4108–4113.
Takeguchi, N., Nakagaki, M., 1969. Biophys. J. 9, 1029–1044.
Tencer, J., Frick, I.M., Oquist, B.W., Alm, P., Rippe, B., 1998. Kidney Int. 53, 709–715.
Tholozan, F.M., Gribbon, C., Li, Z., Goldberg, M.W., Prescott, A.R., McKie, N., Quinlan, R.A., 2007. Mol. Biol. Cell 18, 4222–4231.
Truskey, G.A., Yuan, F., Katz, D.F., 2009. Transport Phenomena in Biological Systems, 2nd ed. Pearson Prentice Hall, Upper Saddle River, N.J.
Uchimura, K., Morimoto-Tomita, M., Bistrup, A., Li, J., Lyon, M., Gallagher, J., Werb, Z., Rosen, S.D., 2006. BMC Biochem. 7, 2.
Venturoli, D., Rippe, B., 2005. Am. J. Physiol. Renal. Physiol. 288, F605–F613.
Walker, J., Menko, A.S., 2009. Exp. Eye Res. 88, 216–225.
Ward, B.W., Notte, J.A., Economou, N.P., 2006. J. Vac. Sci. Technol. B 24, 2871–2874.
Webster Jr., E.H., Searls, R.L., Hilfer, S.R., Zwaan, J., 1987. Anat. Rec. 218, 329–337.
Winkler, J., Wirbelauer, C., Frank, V., Laqua, H., 2001. Exp. Eye Res. 72, 311–318.
Yan, Q., Clark, J.I., Wight, T.N., Sage, E.H., 2002. J. Cell. Sci. 115, 2747–2756.
Yurchenco, P.D., Amenta, P.S., Patton, B.L., 2004. Matrix Biol. 22, 521–538.
Yurchenco, P., Schittny, J., 1990. FASEB J. 4, 1577–1590.